

Effect of Differential Settlements on the Sealing Efficiency of GCLs compared to CCLs: Centrifuge Study

B.V.S. Viswanadham¹, S. Rajesh² and A. Bouazza³

¹Department of Civil Engineering, Indian Institute of Technology Bombay, India;

²Department of Civil Engineering, Indian Institute of Technology Kanpur,

³Department of Civil Engineering, Monash University, Melbourne, Australia

E-mail: viswam@iitb.ac.in

ABSTRACT: Geosynthetic clay liners (GCLs) are being used as an alternative to compacted clays in landfill cover systems because of their very low hydraulic conductivity to water and ease of placement. The main objective of this paper is to examine the performance of GCLs subjected to continuous differential settlements during a centrifuge test at 40 gravities. This paper presents results to two centrifuge model tests, one on clay-based cover system and another on GCL-based cover system. Both models were subjected to an overburden equivalent to that of landfill covers and are instrumented to measure sealing efficiency at the onset of differential settlements. Limiting maximum distortion level at which the barrier system loses its sealing efficiency could be established. For the type of cover systems investigated, the ability of GCL-based cover system to withstand differential settlements without losing their sealing efficiency was found to be superior to that of clay based cover system.

1. INTRODUCTION

1.1 Background

The complete encapsulation of waste can be achieved by providing an impermeable barrier with hydraulic conductivity less than or equal to 10^{-9} m/s as one of the layers in landfill containment systems (Daniel, 1993). The barrier layer may be composed of compacted clays (CCL, Compacted Clay Liner) or geomembranes or Geosynthetic Clay Liners (GCL) or amended soil or the combination of above. In recent times, GCL's are used in many developed countries because of their low hydraulic conductivity (less than or equal to 10^{-11} m/s), ease of installation, increased landfill capacity and limited thickness (LaGatta et al., 1997; Bouazza, 2002; Bouazza et al., 2002). Landfill barriers are prone to fail due to many reasons, out of which, failure due to differential settlements (due to on-going biodegradation of waste) (Ling et al., 1998; Sharma and De, 2007) were emphasized in the present study. Differential settlements are more pronounced in cover systems when compared to bottom lining systems because cover systems are constructed on heterogeneous light weight waste materials. Excessive differential settlements may result in the development of tension cracks in the clay based cover systems along the zone of sharp curvatures thereby resulting in loss of integrity of the whole cover system.

Several investigators modelled the effect of differential settlements on the performance of various clay barriers at the onset of differential settlements (Craig, 1990; Jessberger and Stone, 1991; Scherbeck and Jessberger, 1993; Edelmann et al. 1999; Viswanadham and Mahesh, 2002; Viswanadham and Jessberger, 2005; Viswanadham and Rajesh, 2009; Gourc et al., 2010). From the review of literature, it was found that loss of integrity of clay barrier subjected to the differential settlements was influenced by normal stress resulting from overburden, thickness of the clay barrier, shear strength and the tensile strength characteristics of the clay barrier materials. However, comparison of performance of CCLs with hydrated GCLs while being subjected to differential settlements has not been critically studied. Bredariol et al. (1995) and Edelmann et al. (1999) carried out 1g model tests on the deformation behaviour of GCLs and CCLs, respectively. Edelmann et al. (1999) simulated continuous differential settlements by deflating rubber cushions filled with water below the CCL in large-scale tests. LaGatta et al. (1997) tested five types of in-situ GCL at normal gravity to quantify the relationship between differential settlement and hydraulic conductivity. Differential settlement was simulated by deflating bladder filled with water which produces tensile strains across the short direction of the GCL. It was observed

from the literature review that the clay based hydraulic barrier tends to experience initiation of cracking when the tensile strain developed due to differential settlement is in the range of 0.5 to 1%; severity of cracks increases when the tensile strain is in the range of 1 to 4%. GCL was found to sustain higher differential settlements when compared to CCL (LaGatta et al. 1997). However, the performance assessment of the deformation behaviour of CCLs and GCLs at the onset of differential settlements through centrifuge model testing has not yet been studied extensively. Hence, the focus in the present study is on the performance assessment, through centrifuge tests, of these hydraulic barriers (CCLs and GCLs) when subjected to continuous differential settlement. The centrifuge modelling technique has been adopted to assess the integrity of a model hydraulic barrier which represents the equivalent behaviour in the field. The thickness of the model clay liner material is modelled considering the minimum permissible thickness of the clay barriers present in cover systems which is adopted in various parts of the world, no such issue is relevant to GCLs since they are thin man made materials.

1.2 Centrifuge Modelling

The concept of small-scale model testing to study the physical phenomena is widespread in the engineering field. However, in the geotechnical field, since the stress levels in a small laboratory model are not the same as the stress levels in the full-scale prototype, the small-scale modelling may not simulate the exact field conditions. This problem can be tackled by providing an artificial gravitational field through centrifuge, which makes the stress-strain behaviour of the model identical to that of prototype. The basic principles of centrifuge modelling for geotechnical purposes have been described in detail by Taylor (1995). If the same soil is used in the model and prototype and if a careful model preparation procedure is adopted whereby the model is subjected to a similar stress history ensuring that the packing of the soil particle is replicated, then for the centrifuge model subjected to an inertial acceleration field of N times of the earth's gravity the vertical stress at any depth h_m will be identical to that in the corresponding prototype at depth h_p where $h_p = Nh_m$ (where N is the scale factor or gravity level). Thus, the stress similarity is achieved at homologous points by accelerating a model of scale $1/N$ to N times the Earth's gravity. In order to properly replicate a prototype response in a small-scale model it is necessary to develop scaling relationships, which link the model behaviour to that of the prototype. Scaling laws can be derived by making use of dimensional analysis or from a consideration of the governing differential equations (Langhaar, 1951). The basic scaling

relationships which are used for the present study are summarised in Table 1. The centrifuge tests reported herein were performed at an acceleration field of 40g using a 4.5 m radius beam centrifuge at Indian Institute of Technology Bombay (IIT Bombay). The centrifuge capacity is 2500g-kN with a maximum payload of 25 kNat 100g and at higher acceleration of 200g the allowable payload is 6.25 kN. The detailed specifications are discussed by Viswanadham and Rajesh (2009) and Rajesh and Viswanadham (2012). With the help of an on-board central processing unit (CPU) and other embedded signal conditioning and filter cards available at a large beam centrifuge facility, data was acquired continuously. On-board CPU placed on the swing basket was accessed through a Local Area Network (LAN) connection running through slip rings to the control room situated outside the centrifuge chamber.

Table 1 Summary of scaling relationships in centrifuge modelling

Quantity	Units	Prototype	Model
Length [L]	m	1	#1/N
Area [A]	m ²	1	1/ N ²
Volume [V]	m ³	1	1/ N ³
Acceleration [a]	m/s ²	1	N
Unit weight [γ]	kN/m ³	1	N
Force [F]	kN	1	1/ N ²
Stress [σ]	kN/m ²	1	1
Strain [ε]	%	1	1
Cohesion [c]	kN/m ²	1	1
Angle of internal friction [φ]	degrees	1	1
Time (diffusion) [t]	sec	1	1/N ²
Hydraulic conductivity [k]	m/s	1	N

#L_m/L_p = 1/N; N = Scale factor; m - model; p - prototype;

2. CENTRIFUGE MODEL TESTS ON CCL AND GCL

2.1 Test package

The performance of the CCL and prototype GCL at the onset of differential settlement were analyzed using centrifuge technique. In general, thickness of the CCL varies from 0.6 m to 3 m, although typical thicknesses range between 0.6 m and 1.2 m for cover system. Most of the guidelines suggest that the minimum thickness of compacted clay liner should be 0.6 m (USEPA, 1989; Manassero et al. 1996). Hence, in the present study, 0.6 m thickness of clay barrier was adopted. The response of a 15 mm thick clay barrier tested at 40 g will correspond to a 0.6 m thick clay barrier in the field. Most of the landfill barriers are compacted on the wet side of the compaction curve to achieve low hydraulic conductivity (Benson et al. 1999). In the present case, clay barrier was compacted at OMC + 5%. Generally, the thickness of the cover soil placed above the impervious barrier is about 1.5 m thick (USEPA, 1989). This cover soil may induce overburden pressure close to 25 kN/m². Hence, an overburden of 25 kN/m² was applied at 40 g using 27 mm thick sand layer along with 10 mm free standing water level above the sand layer for all the tests. Two centrifuge tests were performed in the present study, one for each hydraulic barrier (CCL and GCL) at 40g. The testing has been carried out for identical gravity level, magnitude of settlements, settlement rates, dimensions of barriers and surcharge.

2.2 Model materials

2.2.1 CCL

Benson et al. (1999) developed a database comprising of 85 active landfills in USA. It was reported that in most of the landfill sites, the clay barrier placed in cover systems present in has liquid limit ranging from 30 - 40% and plasticity index ranging from 10 – 20%. Most of the clay barriers are compacted on the wet side of optimum (standard Proctor). In the present study, it was decided to model the compacted clay which has the above mentioned properties such that

it represents a wide spectrum of material characteristics of clay barriers of landfill cover systems. Various kaolin-sand blends were tried to achieve the ideal properties of landfill barrier material; out of which kaolin-sand mix of 4:1 by dry weight was chosen as a model barrier material. The properties of model barrier materials are presented in Table 2.

Table 2 Properties of model CCL material

Properties	Values
Hygroscopic moisture content [%]	0.9
Specific gravity	2.54
Liquid limit [%]	38
Plasticity index [%]	16
Maximum dry unit weight [kN/m ³] (Standard Proctor)	15.9
Optimum moisture content [%] (Standard Proctor)	22
Cohesion [kN/m ²]	38
Angle of internal friction [°]	15
Coefficient of permeability [m/s]	0.4 x 10 ⁻⁹

2.2.2 GCL

In the present study, a sodium bentonite based prototype GCL was used. As per the testing requirement, a GCL specimen of 720 mm long, 450 mm wide and 6 mm thick in dry state was supplied. The GCL was allowed to hydrate under a normal stress of 25 kPa for about 96 hours, such that its final thickness was approximately 15 mm. The properties of GCL are reported in Table 3.

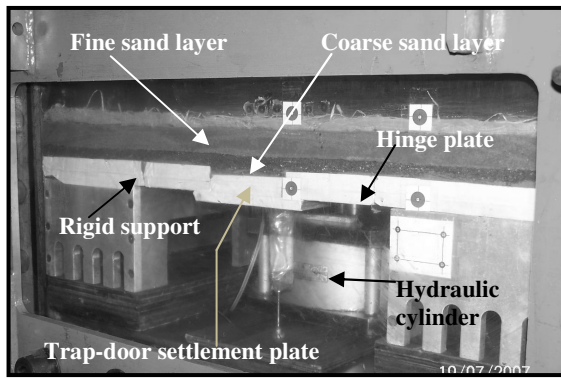
Table 3 Properties of prototype GCL material

Properties	*Values
Product code	NaBento
Geotextile carriers	Woven [PP]
Weave type	Needle-punched
Sealing layer	Sodium- bentonite
Unit weight [g/m ²]	4800
Thickness in dry condition [mm]	6.0
Ultimate tensile strength [kN/m]	
Longitudinal	≥ 22
Transverse	≥ 30
Strain at nominal tensile strength [%]	
Longitudinal	≤ 25
Transverse	≤ 30
Coefficient of permeability [m/s]	5 x 10 ⁻¹¹

*As supplied by the manufacturer

2.3 Testing Methodology

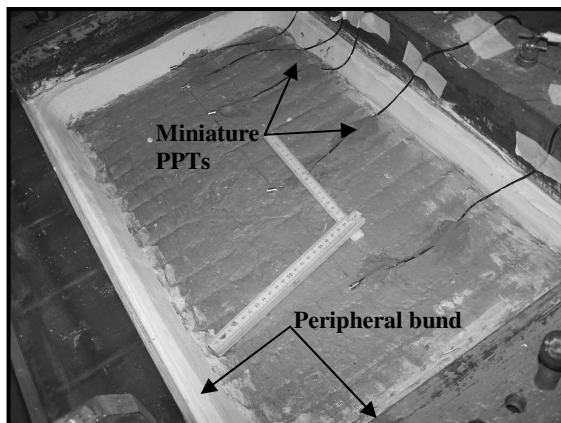
The various stages involved in the preparation of centrifuge model test are shown in Fig. 1. Response of hydraulic barriers to differential settlement was simulated symmetrically by sinking the hydraulic trap-door arrangement, as shown in Fig. 2; detailed explanation of the set-up was discussed by Viswanadham and Rajesh (2009). Hydraulic trap-door arrangement comprises a hydraulic cylinder, potentiometer, trap-door settlement plate, two rigid supports and two hinge plates with a hinge connection. The hinged plates were made to rest on a trap-door settlement plate connected to a hydraulic cylinder symmetrically, as shown in Fig. 1a. When the hydraulic cylinder is in full-stroke, horizontal plane can be achieved. The model was prepared at normal gravity (1g) with the cylinder at its full stroke under an operating pressure of 400 kN/m² and the flow control valves were kept closed and oil in the trap-door cylinder was not allowed to move out to prevent premature settlements to the model hydraulic barrier, if any.



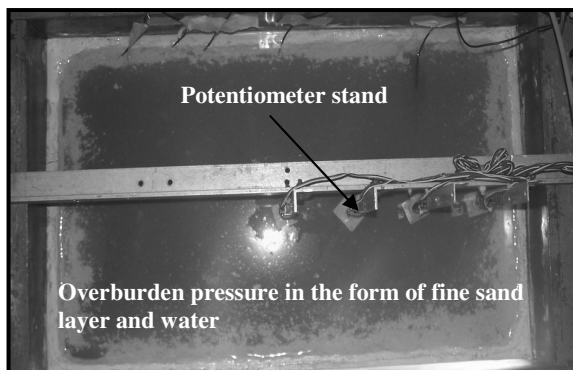
a) Component of Hydraulic trap-door system



b) Placement of saturated prototype GCL and gluing discrete markers



c) Placement of sealing layer and peripheral bunds



d) Connection of various sensors with computer controlled data acquisition system

Figure 1 Various stages involved in the preparation of centrifuge model test [Model: GCL]

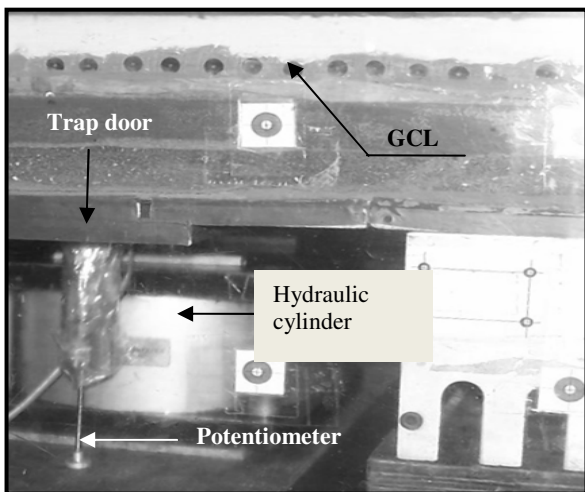
A strong box (container) having internal dimensions of 720 mm x 450 mm x 410 mm was used in the present study. The entire test setup was placed inside the strong box. After making the levelled platform, a thick non-woven geotextile layer cut into three pieces was placed along the length of the container. A 30 mm thick coarse sand layer followed by 30 mm thick fine sand layer were placed in dry state by pluviation technique at a relative density of 55% (Fig. 1a). The geotextile, coarse and fine sand layers were introduced to eliminate any stress concentration, which may arise due to abrupt discontinuity at hinge locations and are referred herein as sacrificial layers. The sand layers were pre-saturated and drained for about 9 – 10 hours in 1g condition. The 15 mm thick CCL (0.6 m thickness at 40g) was prepared by mixing the kaolin and sand in the ratio of 4:1 and moist-compacted at a moulding water content of OMC + 5% with the corresponding dry unit weight (14.2 kN/m³) using standard Proctor compaction test results. In the case of GCL testing, the saturated GCL was placed above the scarifying layer without any slack, as shown in Fig. 1b.

Discrete markers were inserted along the cross-section at every 20 mm centre to centre distance and 3 mm below the top surface of the model CCL to measure integral displacements of these markers during various stages of the test. In the case of GCL, markers were glued onto top geotextile layer using an epoxy adhesive (Fig. 1b). A stiff bentonite paste was applied all around the barrier to limit the infiltration of water along the interface of barrier and container. A peripheral bund was formed all around the barrier using the blend of kaolin and sand in the ratio of 4:1, as shown in Fig. 1c to ensure adequate anchorage to the GCL. A series of five numbers of Pore Pressure Transducers (PPT) were placed above the properly prepared barriers, as shown in Fig. 1c, to measure the water breakthrough and the time at which the integrity of the barrier was lost. After placing the PPT's in position, surcharge pressure equivalent to 25 kN/m² at 40g was created using 27 mm thick saturated sand layer and with a water height of 10 mm above the sand surface. Four numbers of potentiometers were placed on the right half cross-section of the barrier at every 100 mm interval starting from the centre line of the barrier, as shown in Fig. 1d. ChargeCoupled Device (CCD) video camera, was placed on the front side of the model to monitor the performance of the barrier during the centrifuge test.

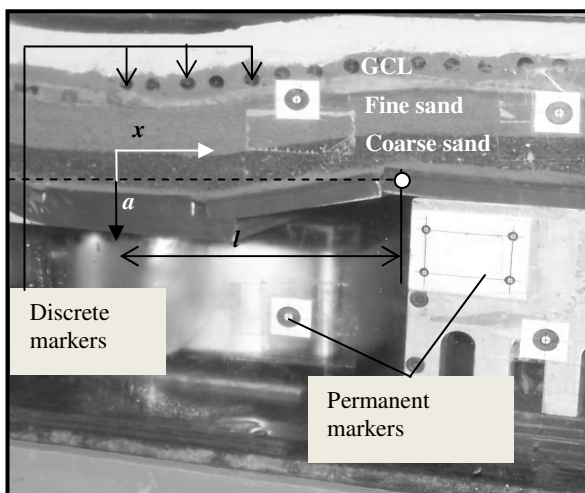
The front elevation of the test-setup at the onset of differential settlement during centrifuge test is shown in Fig. 2a. After placing all soil layers and connecting all the PPT's, and potentiometers to an onboard data acquisition system, the centrifuge was directly set to 40g acceleration by rotating at a constant angular velocity of 93 rpm and waited for about 10 minutes to establish equilibrium of the entire system. While increasing the gravity level from 1g to 40g, air pressure was increased from 400 – 500 kN/m² gradually to prevent any premature movement of the trap-door plate. After completing the waiting period, the air pressure within the oil tank was slowly reduced in steps for maintaining a constant rate of settlement of the trap-door cylinder assembly. Desired settlement control rate was achieved by withdrawing the air pressure in the tank (located behind the container on a swing basket) in steps and allowed the oil to flow out of the cylinder through a needle flow control valve. The model test package has been calibrated beforehand to obtain a fixed rate of settlement. On an average, a settlement rate of 0.85 mm/min (in model dimensions) was achieved for all the tests and differential settlements were induced continuously. The miniature potentiometer attached to the trap-door plate was used to monitor the movement of the trap-door plate, which would provide the central settlement a values starting from zero to a maximum of 25 mm in model dimensions (1 m in prototype dimension) during the centrifuge test. Figure 2b shows the status of the prototype GCL at a central settlement of 1 m.

Differential settlement may be characterized by the distortion level a/l , which is defined as settlement a , over a horizontal distance l (Fig. 2b). Use of distortion level for characterizing differential settlement was adopted earlier by LaGatta et al. (1997). For the developed test package configuration, a distortion level a/l (i.e.

a_{max}/l) up to 0.125 could be imposed to the barrier during centrifuge test. When the horizontal distance from centre of the barrier x is zero, the value of settlement is defined as central settlement represented as a and is referred herein as maximum central settlement a_{max} , if the induced central settlement equals to 25 mm or achieved central settlement during penultimate stages of centrifuge test (in model dimensions), whichever is greater. At the various stages of central settlements, photographs were taken through image acquiring software and were later used for image analysis to compute deformation profiles and for arriving at outer fibre strain distribution along the top fibre of the barriers tested. After attaining a maximum central settlement a_{max} equal to 25 mm at 40g corresponding to a central settlement of (1 m in the prototype), the air pressure in the tank was released to zero to prevent bouncing of the hydraulic cylinder piston while centrifuge was stopped.



a) Before inducing differential settlement



b) After inducing differential settlement

Figure 2 Deformation of the GCL before and after subjected to differential settlements. [Model: GCL]

3. ANALYSIS AND INTERPRETATION OF CENTRIFUGE TEST RESULTS

3.1 Deformation profiles

The deformation profiles can be obtained by potentiometers and Digital Image Analysis. Since in the present study, the potentiometers were placed at a spacing of 100 mm centre to centre, the accuracy of the deformation profiles through potentiometers was not achieved. Hence, markers were used to arrive at deformation

profiles by performing digital image analysis of photographs retrieved during various stages of centrifuge model test. The digital image analysis was carried out using high quality pictures captured at various stages of the central settlements using GRAM++ software (GRAM++, 2008). The four permanent markers, whose coordinates are predefined, are fixed on the inner side of Perspex glass (refer Fig. 2a). The coordinates of the discrete markers were determined with reference to the coordinate of the permanent markers using map edit module of GRAM++. The variation of actual movement of the discrete markers at every stage of central settlement was determined with reference to the zero central settlement. The measured co-ordinates of a row of markers fixed in the soil in all settlement stages are approximated with an exponential equation of the normal distribution to get the deformation at various stages, curvature and strain computations along the longitudinal axis of the clay barrier (Sengupta, 2005). The variation of deformation profiles of CCL and GCL at different stages of central settlement is shown in Fig. 3. Keeping in view of the symmetry, only the right hand portion of the GCL was shown. A smooth variation in the deformation profiles along the length of both barriers can be noticed for all the ranges of central settlement. It can be noticed that GCL tends to deform more compared to the CCL up to the location of the hinge location; however, beyond the hinge location both barrier tends to have identical variation (negligible deformation).

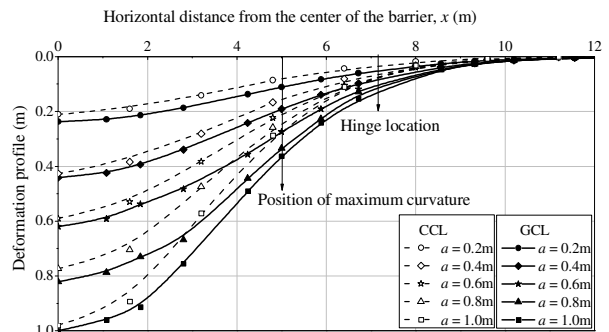


Figure 3 Variation of deformation profiles with horizontal distance [Model: GCL]

3.2 Strain computation

The elongation strain (ϵ_l) is related to the in-plane deformations of the clay or GCL barrier. It is assumed constant throughout the thickness of the barrier. Bending strain (ϵ_b) or curvature strain is not constant throughout the thickness and varies along the horizontal distance and its depth. In case of bending strain, neutral layer has zero strain, while the top and bottom fibres have tensile and compressive strains respectively. Outer fibre strain (ϵ_{of}) is the summation of the elongation and the curvature strain. If $w(x)$ is the function of deformation profile of the barrier and $w'(x)$ and $w''(x)$ are the first and second derivatives of $w(x)$, then the strains can be computed using combined bending and elongation method (Tognon et al., 2000). Elongation strain is the strain due to change in length which can be approximately obtained from $w'(x)$. Bending strain is the strain due to change in curvature which can be computed using $\epsilon_k(x) = R_{of} \kappa(x) d$; where, $\kappa(x)$ is the curvature of the soil barrier along the horizontal distance x , which is equal to $[1/R(x)]$ and is equal to $w''(x)$, second derivative of $w(x)$; and $R(x)$ is the curvature radius of the soil barrier along the horizontal distance x , R_{of} is the neutral layer coefficient which is taken as 0.667 (Lee and Shen, 1968), d is the thickness of the soil barrier. The outer fibre strain distribution for the GCL model along the horizontal distance from the centre of the barrier is shown in Fig. 4. It can be observed that as the central settlement increases, the strain values also increase. When the strain value increases beyond the permissible value of the barrier material, then there may be an occurrence and propagation of the cracks which may hamper the functionality of the cover system.

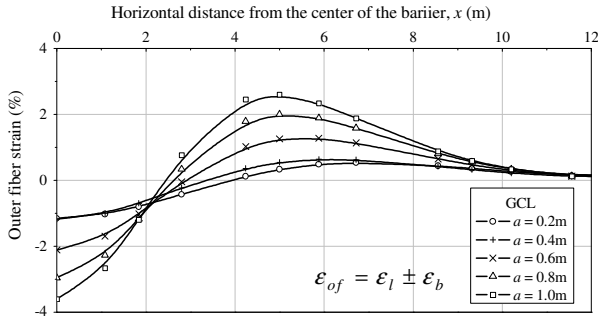


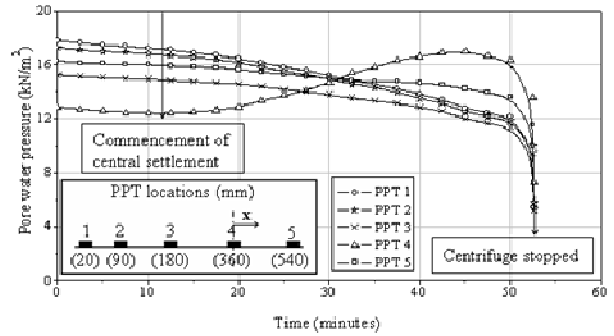
Figure 4 Variation of outer fibre strain with horizontal distance from the center of GCL

3.3 Water breakthrough analysis

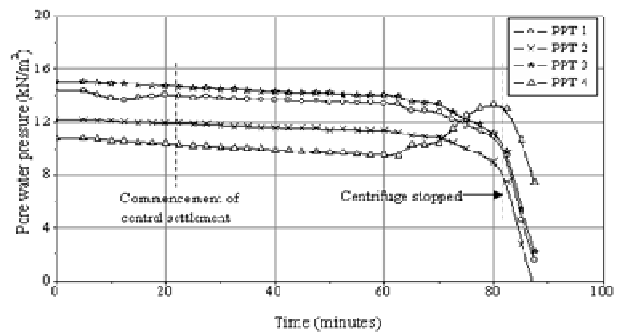
The severity of the water breakthrough and the integrity of the tested barrier at the onset of differential settlements were analysed in this study, with the help of known volume of water stored above the barrier surface. The performance of the barrier as an effective sealing layer can be best illustrated through infiltration rate or permeant flow through the barrier. In the present study, tap water was used as permeant. This infiltration rate can be directly observed by the reduction in the volume of the water at every stage of centrifuge testing. The change in volume of the water can be determined using the change in water levels measured using PPTs, installed at the top surface of the barrier placed at mid-width of the container. By keeping symmetry in to consideration, PPTs are placed on one half of the container. A special type of miniature PPTs (PDCR81 manufactured by General Electric, UK) were used to measure water levels above the barrier surface (Viswanadham and Rajesh, 2009). Location of the PPTs is shown in the inset of Fig. 5. PPTs used for the analysis are calibrated and soaked in water for more than 48 hours prior to testing. The water pressure above the mid height of PPT can be obtained from PPT measurements at different locations and at various settlement stages. Variation of the pore water pressure with time, for the model CCL and GCL is shown in Fig. 5.

As the central settlement was induced the barrier tends to deform, which in turn make the water to accumulate at the central portion of the model barrier. This can be clearly observed as an increasing trend in the pressure from PPT 4 which is in contrast with other PPTs. From the pore water pressure measurements, the height of water present above every PPTs can be determined. Initial height of the water present at various locations was determined, before the commencement of trap-door movements. The area under measured water profile (i.e., through numerical integration) can provide volume per unit width of water. The height of water along the width of the container was assumed to be identical to that of the height of water measured at the mid-width of the container. Hence, the volume of the water present above the model barrier (on one half) can be computed by the product of the volume per unit width of the water to that of the width of the container. Total volume of water is the twice of the volume of water computed for one half section. The change in volume of water at any settlement stage can be determined by the numerical difference between the initial volume of water to the volume of water at the required settlement stage. Volume change ratio which is defined as ratio of volume of water at any instance (V) to the initial volume of water (V₀). Typical values of volume change ranges from 1 to 0. Complete infiltration of water through the barrier is attained whenever V/V₀ tends to 0. At a = 0 mm, value of volume change ratio will be one whereas as if there is any change in the volume due to infiltration of the water into the barrier then its value will be less than one. However, it can be observed from Fig. 5 that pore water pressure at all the locations was almost constant before the commencement of central settlement. If the sealing arrangement provided all around the barrier

is intact, volume of water reduction can only be due to infiltration of water into the barrier.



a) Model CCL

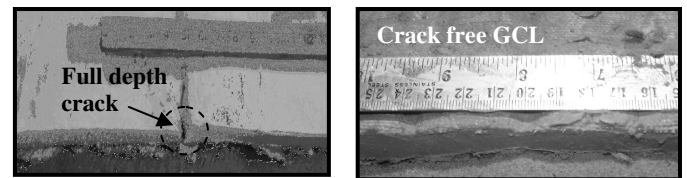


b) Model GCL

Figure 5 Variation of pore water pressure with time (Time is in model dimensions)

4. RESULTS AND DISCUSSION

The performance of 0.6 m thick CCL and a prototype GCL at the onset of differential settlement were analysed by conducting centrifuge model test at 40g. The comparisons were made in terms of strains, radius at the zone of maximum curvature, volume change ratio at various distortion levels and limiting distortion level corresponding to water breakthrough for both barriers. Figure 6 shows the status of CCL and GCL after being subjected to a distortion level of 0.125. A clear distinct wide full-depth crack can be noticed for the CCL. However, crack free GCL can be noticed even after inducing distortion level of 0.125. This shows the significant improvement in the deformation behaviour of GCL when compared to CCL.



a) Model CCL

b) Model GCL

Figure 6 Status of both barriers at the zone of maximum curvature after being subjected to a distortion level of 0.125

Maximum outer fibre strain computed for GCL and CCL model are shown in Fig. 7. It can be observed that as the distortion level increases, the maximum outer fibre strain of both barriers increases. It can also be observed that up to a settlement ratio of 0.6 (distortion level of 0.075) variation of maximum outer fibre strain with settlement ratio has a gentle slope, whereas, when it exceeds 0.6, gentle slope changes to considerable steep slope. This variation can be seen in both the barriers. For the maximum central settlement of

1 m, it can be observed that the barriers experience a maximum outer fibre strain at the zone of maximum curvature in the range of 2.8 to 3%.

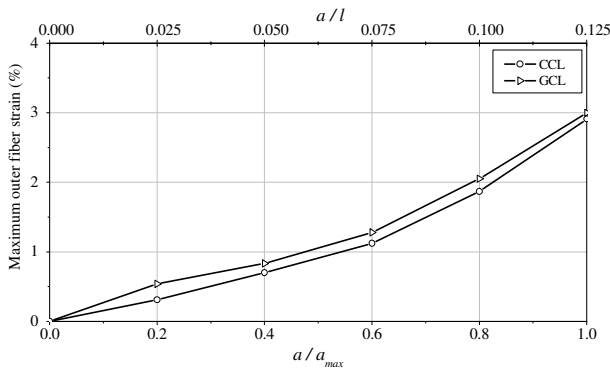


Figure 7 Variation of maximum outer fibre strain at the zone of maximum curvature with a/a_{max} and a/l

Figure 8 shows the comparison of the variation of volume change ratio with settlement ratio and distortion level for both barrier types tested in the present study. It can be observed that there exists a gentle variation of volume change ratio up to certain settlement ratio followed by a steep variation. Limiting distortion level corresponding to water breakthrough can be quantified by double integration method, as shown in Fig. 8. The limiting distortion level for CCL and GCL was found to be 0.068 and 0.095 respectively. A sudden decrease in the value of V/V_0 can be observed when the distortion level approaches 0.068 for CCL. This implies that barrier could have experienced the initiation and propagation of crack extensively such that up a complete loss of integrity of the barrier has occurred before the distortion level reaches limiting distortion level. Hence, limiting distortion level indicate the maximum permissible distortion level allowed for a particular barrier material to avoid complete loss of integrity in terms of water intactness.

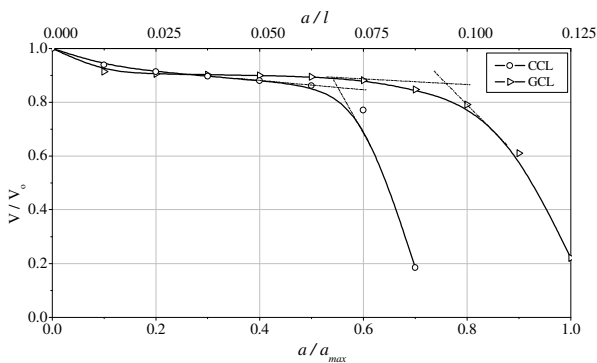
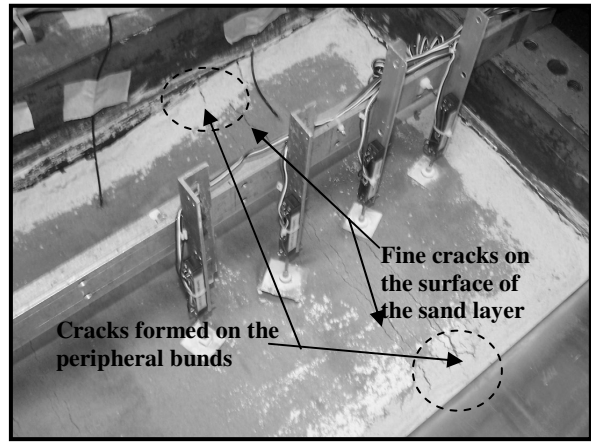


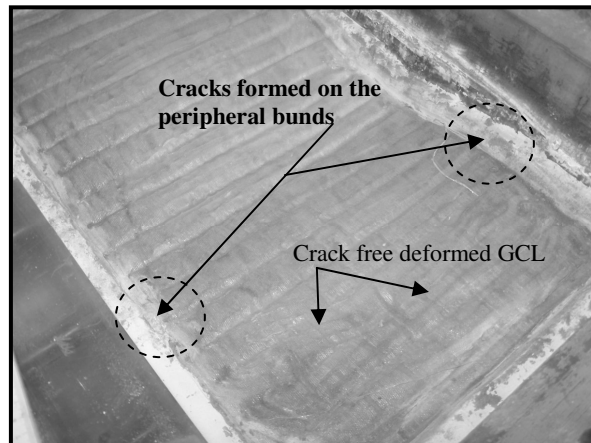
Figure 8 Variation of volume change ratio with a/a_{max} and a/l .

For both barrier tests, identical water sealing arrangement has been provided in the form of thick bentonite paste and peripheral bunds all around the interface between the barrier and the container (refer Fig. 1c) such that infiltration of water may only be possible either due to pore spaces present in the barrier or due to crack formation. From the post-test examination of deformed barrier (CCL), intactness of sealing arrangement was checked. Hence, the volume change observed in Fig. 8 was due to the infiltration of water through barrier. However, for the GCL case, GCL was found to be intact from the post-test investigation (refer Fig. 6b) but the peripheral bunds were cracked, as shown in Figs. 9a and 9b because of higher distortion level. The reduction in the value of V/V_0 could be mainly due to the infiltration of water through the cracks experienced on peripheral bunds. Even if the GCL tend to crack at the worst situation, cracks can be closed due to the self-healing

nature of bentonite present in the GCL. The results from the present study were found to be in agreement with those reported earlier by LaGatta et al. (1997). From the present study, it can be noticed that performance of deformation behaviour of GCL was found to be many times greater than conventional CCL.



a) GCL with fine sand layer at a distortion level of 0.125



b) Top view of exposed GCL after removing sand layer

Figure 9 Snaps showing cracks on peripheral bund and fine sand layer [Model: GCL]

4.1 Scale effect and limitation

Since the problem related to deformation behaviour of barriers at the onset of differential settlement is a stress related problem, the body forces plays an important role. Hence, small-scale model tests at 1g may not represent the actual field conditions. To overcome this problem, either full scale model testing or centrifuge testing are essential. As the full scale field testing involves higher cost and time, centrifuge modelling may be the ideal solution to tackle the above mentioned problem. Centrifuge modelling technique is now firmly established as a dependable research tool that can provide solutions to many of the hitherto intractable problems in geotechnical engineering. In order to assess and compare the performance of various barrier materials at the onset of differential settlements, model CCL barrier material, thickness of the barrier and the overburden pressure were selected considering relevant scaling laws for centrifuge testing. As the prototype GCL is of very low thickness (6 mm in dry state) and the scaling law governing modelling GCL in centrifuge testing is not yet established, prototype GCL was used in the present study. In centrifuge, prototype GCL may provide higher resistance to the deformation when compared to the model GCL. Hence, it may not really replicate the exact behaviour of GCL in the field. Modelling of GCL according to

centrifuge scaling considerations and testing it at suitable enhanced gravities may be an interesting topic of research to know the exact behaviour of GCL at the onset of differential settlement.

5. CONCLUSIONS

The performance of CCL and GCL at the onset of differential settlements was analysed using centrifuge technique at 40g. Controlled in-flight simulation of non-uniform settlements of landfill in a geotechnical centrifuge was carried out using trap-door arrangement. Digital image analysis technique was found to be very useful in arriving at deformation profiles and strain distribution along hydraulic barriers subjected to differential settlements. Based on the analysis and interpretation of centrifuge test results, following conclusions can be drawn:

- a) Compacted clay liner of 0.6 m thickness on wet side of optimum (OMC + 5%), experienced full-depth crack when settlement ratio attained a value of 0.55. Width and depth of the cracks were large enough to allow the water when a settlement ratio of 0.7 was reached. Up to a settlement ratio of 0.5, the variation in the hydraulic conductivity of the CCL was found to be marginal, thereafter a drastic increase was observed once settlement ratio increased beyond 0.6. Limiting maximum distortion level of 0.068 was registered for CCL subjected to differential settlements. At this distortion level, considerable water flow through CCL was observed.
- b) For a prototype GCL, even after inducing distortion level of 0.125, the tested barrier was found to be free from any cracks. Limiting maximum distortion level of 0.095 was registered for the type of GCL tested, which is about 40 % superior to CCL. This improved response of GCL to the differential settlements is attributed to compatibility of saturated nature of fibre blended bentonite and upper and lower carrier geotextiles. This study suggests that GCL used in the present study appears to have the ability to maintain the desired hydraulic conductivity and sustain large differential settlements anticipated in landfill cover systems.

6. ACKNOWLEDGEMENTS

The authors would like to thank Centrifuge staff at the National Geotechnical Centrifuge Facility of IIT Bombay for their untiring support throughout the present study. Thanks are also due to M/s Huesker GmbH, Germany for supplying the GCL used in the present study.

7. REFERENCES

Benson, C. H., Daniel, D. E., and Boutwell, G. P. (1999). "Field performance of compacted clay liners". *J. Geotech. and Geoenviron. Engrg.*, ASCE, 126, Issue 5, pp 390-403.

Bouazza, A. (2002). "Geosynthetic clay liners". *Geotextiles and Geomembranes*, 20, Issue 1, pp 1-17.

Bouazza, A., Zornberg, J. G. and Adams, D. (2002). "Geosynthetics in Waste Containment Facilities: Recent Advances". *Proceedings of the 7th International Conference on Geosynthetics*, Nice, France, Volume 2, pp 445-507.

Bredariol, A. W., Martin, J. P., Cheng, S., and Tull, C. F. (1995). "Flexural cracking of compacted clay in landfill covers". *Geoenvironment 2000, Geotechnical Special Publication No. 46*, ASCE, Y.B. Acar and D. E. Daniel (Eds.), Volume 1, pp 914-931.

Craig, W. H. (1990). "Collapse of cohesive overburden following removal of support". *Can. Geotech. J.*, 27, Issue 3, pp 355-364.

Daniel, D. E. (1993). "Geotechnical Practice for Waste Disposal". Chapman & Hall, London.

Edelmann, L., Hertweck, M., and Amann, P. (1999). "Mechanical Behaviour of Landfill Barrier Systems". *Proc. Instn. Civ. Engrs, Geotech.Engg.* 137, Issue 4, pp 215-224.

Gourc, J. P., Camp, S., Viswanadham, B. V. S., and Rajesh, S. (2010). "Deformation behaviour of clay cap barriers of hazardous waste containment systems: full-scale and centrifuge tests". *Geotextiles and Geomembranes*, 28, Issue 3, pp 281-291.

GRAM++, 2008. "Technical document". CSRE, Indian Institute of Technology Bombay <http://www.csre.iitb.ac.in/gram++/>.

Jessberger, H. L., and Stone, K. J. L. (1991). "Subsidence effect on clay barriers". *Geotechnique*, 41, Issue 2, pp185-194.

Jessberger, H. L. (1994). "Geotechnical aspects of landfill design and construction. Part 1, Part 2 and Part 3". *Proc. Instn. Civ. Engrs, Geotech.Engg.*, 107, Issue 2, pp 99-122.

Langhaar, H. L. (1951). "Dimensional analysis and theory of models", John Wiley, New York.

LaGatta, M. D., Boardman, B. T., Cooley, B. H., and Daniel, D. E. (1997). "Geosynthetic clay liners subjected to differential settlement". *J. Geotech. and Geoenviron. Engrg.*, ASCE, 123, Issue 5, pp 402-410.

Lee, K. L., and Shen, C. K. (1969). "Horizontal movements related to subsidence". *Journal of Soil Mech. and Found. Div.*, ASCE, 94, Issue 6, pp139-166.

Ling, I., Leshchinsky, D., Yoshiyuki, M., and Toshinori, K. (1998). "Estimation of municipal solid waste landfill settlement". *J. Geotech. and Geoenviron. Engrg.*, ASCE, 124, Issue 1, pp 21-28.

Manassero, M., Van Impe, W. F., and Bouazza, A. (1996). "Waste disposal and containment". *Proceedings 2nd Int. Congr. on Environmental Geotechnics*, Osaka, Japan, Balkema, Rotterdam, The Netherlands, Pedro S. Seco e Pinto (ed), Volume 3, pp 1425-1474.

Rajesh, S., and Viswanadham, B.V.S. (2012). "Modelling and instrumentation of geogrid reinforced soil barriers of landfill covers". *J. Geotech. and Geoenviron. Engrg.*, ASCE, 138, Issue 1, pp 26-37.

Scherbeck, R., and Jessberger, H. L. (1993). "Assessment of deformed mineral sealing layers". *Proceedings of Waste disposal by Landfills - Green' 93*, London, R.W. Sarsby (ed), Balkema, pp. 477-486.

Sengupta, S. S. (2005). "Modeling deformation behaviour of compacted soil liners in a geotechnical centrifuge". *Masters of Technology dissertation*, Indian Institute of Technology Bombay, India.

Sharma, H.D., and De, A. (2007). "Municipal Solid Waste Landfill Settlement: Postclosure Perspectives". *J. Geotech. and Geoenviron. Engrg.*, ASCE, 133, Issue 6, pp 619-629.

Taylor, R. N. (1995). "Centrifuges in modelling: principles and scale effects". *Geotechnical Centrifuge Technology*, Blackie Academic and Professional, Glasgow, U. K., pp. 19-33.

Tognon, A. R., Rowe, R. K., and Moore, I.D. (2000). "Geomembrane strain observed in large-scale testing of protection layers". *J. Geotech. and Geoenviron. Engrg.*, ASCE, 126, Issue 12, pp 1194-1208.

USEPA, (1989). "EPA technical guidance document: Final covers on hazardous waste landfills and surface impoundments", EPA/530- SW-89-047. U.S. Environmental Protection Agency, Washington, D.C.

Viswanadham, B. V. S. and Mahesh, K. V. (2002). "Modeling deformation behaviour of clay liners in a small centrifuge". *Can. Geotech. J.*, 39, Issue 6, pp 1406-1418.

Viswanadham, B. V. S. and Jessberger, H. L. (2005). "Centrifuge modeling of geosynthetic reinforced clay liners of landfills". *J. Geotech. and Geoenviron. Engrg.*, ASCE, 131, Issue 5, pp 564-574.

Viswanadham, B.V.S. and Rajesh, S. (2009). "Centrifuge model tests on clay based engineered barriers subjected to differential settlement". *Applied Clay Science*, 42, Issues 3-4, pp 460-472.